Chinese Journal of Aeronautics, (2018), 31(7): 1525–1534

Chinese Society of Aeronautics and Astronautics
& Beihang University

Chinese Journal of Aeronautics

cja@buaa.edu.cn
www.sciencedirect.com

Evaluation of mixed mode-I/II criteria for fatigue crack propagation using experiments and modeling

Oğuzhan DEMIR [a,b], Ali O. AYHAN [a,*], Sedat IRIC [a], Hüseyin LEKESIZ [c]

[a] Department of Mechanical Engineering, Sakarya University, Sakarya 54187, Turkey
[b] Department of Mechanical Engineering, Bilecik Şeyh Edebali University, Bilecik 11210, Turkey
[c] Department of Mechanical Engineering, Bursa Technical University, Bursa 16310, Turkey

Received 31 July 2017; revised 25 December 2017; accepted 18 March 2018
Available online 18 May 2018

KEYWORDS

Crack propagation;
Fatigue crack growth simulation;
Fatigue crack growth test;
Fracture mechanics;
Mixed mode-I/II

Abstract In this study, in-plane mixed mode-I/II fatigue crack growth simulations and experiments are performed for the Al 7075-T651 aluminum alloy which is widely used in the aerospace industry. Tests are carried out under different mode mixity ratios to evaluate the applicability of a fracture criterion developed in a previous study to mixed mode-I/II fatigue crack growth tests. Results obtained from the analyses and experiments are compared with existing and developed criteria in terms of crack growth lives. Compact Tension Shear (CTS) specimens, which enable mixed mode loading with loading devices under different loading angles, are used in the simulations and experiments. In an effort to model and simulate the actual conditions in the experiments, crack surfaces of fractured specimens are scanned, crack paths are modeled exactly, and contacts are defined between the contact surfaces of a specimen and the loading device for each crack propagation step in the analyses. Having computed the mixed mode stress intensity factors from the numerical analyses, propagation life cycles are predicted by existing and the developed mixed mode-I/II criteria and then compared with experimental results.

1. Introduction

Fracture mechanics and its applications, including mixed-mode fracture, are being studied extensively in such important areas as energy, defense, aviation, and space industries in developed countries that produce high-technology products. Fracture and crack propagation analyses are performed for airframe, helicopter, and aircraft engine parts even during the design phase. Many of the fracture and fatigue crack propagation problems that have been encountered in the aviation industry are related to fuselage of military and passenger aircraft, gas turbine engines and turbine blades.[1–13]

Fatigue crack growth studies for many practical engineering problems have mostly concentrated on pure mode-I loading condition over the past six decades. Unfortunately, pure mode-I loading condition does not always occur in practice, and in many cases, cracks are exposed to mixed mode loads, i.e., directions of the loads are not normal to the crack plane.

* Corresponding author.
E-mail address: ayhan@sakarya.edu.tr (A.O. AYHAN).
Peer review under responsibility of Editorial Committee of CJA.

ELSEVIER Production and hosting by Elsevier

https://doi.org/10.1016/j.cja.2018.05.009

During crack growth under mixed mode loading, crack growth direction changes in accordance with mode mixity ratios. Thus, for accurate assessment of life predictions, crack growth direction plays a key role along with the fatigue crack growth rate under mixed mode loading conditions. Mixed mode fracture and crack propagation problems are encountered due to different reasons: multi-axial and mixed mode loads, non-perpendicular orientations of crack surfaces with respect to global uniaxial loading, and different types and combinations of boundary conditions.

Several stress- or energy-based fracture criteria have been proposed so far to understand the fracture mechanism of in-plane mixed mode problems. Maximum Tangential Stress (MTS),[14] minimum Strain Energy Density (SED),[15] Maximum Energy Release Rate (MERR)[16,17] and Maximum Tangential Strain (MTSN)[18] criteria are some of the most common theoretical criteria used in fracture and crack propagation analyses for mixed mode-I/II fracture problems. Tanaka,[19] Richard[20–22] and Pook[23] et al. also proposed different fracture criteria by defining equivalent Stress Intensity Factor (SIF) equations. For predictions of the crack growth increment and direction under in-plane mixed mode loading, definition of an equivalent SIF representing a combination of mode-I and mode-II SIFs is essential. Although many criteria have been proposed with regard to predictions of crack growth increment and its direction for mixed mode-I/II fracture problems, there is no standard criterion for mixed mode crack growth tests. Biner[24] investigated the crack growth behavior of AISI-304 stainless steel under mixed mode-I/II loading conditions by using Compact Tension Shear (CTS) specimens, and compared experimental crack growth directions with those obtained using the SED criterion and the MERR criterion. The author reported that the SED criterion significantly over-estimates the deflection angle of crack growth at high mode mixities. Zafosnik et al.[25] also performed mixed mode-I/II crack growth simulations and tests using CTS specimens made of Al alloy and results obtained from simulations combined with MTS and SED criteria were compared with experimental data. The results showed that, as is the case with Biner's results, the SED criterion is less accurate for determination of the kink angle under high mode mixities, and the MTS criterion provides good prediction agreement, but for further crack extensions the criterion deviates from experimental data. A literature survey about various criteria proposed for predictions of mixed mode crack growth directions and rates was given by Qian and Fatemi.[26] They reported by referring to studies existing in the literature that significant discrepancies occur between crack growth criteria when the mode-II component is dominant under mixed mode-I/II loading conditions. Ren et al.[27] reviewed several widely accepted fracture criteria in terms of crack initiation angle and fracture toughness ratio under in-plane mixed mode fracture. The authors indicated that many criteria can provide a good prediction for predominately mode-I fractures, but none of them yields good predictions under predominately mode-II conditions. In a previous paper,[28] mixed mode-I/II fracture analyses and experiments were performed for different types of CTS specimen, and data obtained from the experiments was compared with predictions from the analyses using existing criteria in the literature. Results showed that existing criteria yield reasonably close predictions to those of experiments for up to moderate levels of mode mixity in the loading. However, most existing criteria start deviating from experimental measurements for highly mixed mode loading conditions. Therefore, using all data obtained from analyses and experiments, improved empirical mixed mode-I/II fracture criteria were proposed in terms of fracture loads and crack deflection angles, and the developed criteria[28] were validated by applying them to the results of the experiments. Although the previous study[28] focused on mixed-mode fracture toughness tests under static loading, in this study, fatigue crack growth modeling and experiments are performed to validate the developed equivalent SIF equation in terms of propagation life cycles. In this context, in-plane mixed mode-I/II fatigue crack growth experiments are performed by using CTS specimens. Fracture surfaces of broken specimens are modeled exactly by scanning the surfaces, and fracture analyses are performed by simulating the real conditions in the experiments for all crack growth increments of the tests. Having computed the mixed mode stress intensity factors from the numerical analyses, equivalent SIFs on the crack fronts are calculated using existing and developed criteria, and life cycles are computed for each criteria. Finally, crack growth lives under different loading angles (30°, 45°, 60° and 75°) are compared with experimental results.

2. Existing in-plane mixed mode criteria

For determination of fracture behaviors under in-plane mixed mode loading conditions, there are various criteria that exist in the literature. Some of these criteria are summarized in this section.

The Erdogan and Sih criterion[14] is one of the most commonly used criterion for in-plane mixed mode problems. According to this criterion, crack propagates from the crack tip radially at a direction which contains the maximum tangential stress. If this tangential stress exceeds a critical value or an equivalent stress intensity factor (K_{eq}) reaches the fracture toughness (K_{IC}) value of the material, crack propagation becomes unstable, and fracture occurs. K_{eq} and the crack deflection angle for this criterion are expressed by

$$K_{eq} = \cos\frac{\phi_0}{2}\left[K_I \cos^2\frac{\phi_0}{2} - \frac{3}{2}K_{II}\sin\phi_0\right] = K_{IC} \tag{1}$$

$$\phi_0 = -\arccos\left(\frac{3K_{II}^2 + K_I\sqrt{K_I^2 + 8K_{II}^2}}{K_I^2 + 9K_{II}^2}\right) \tag{2}$$

where K_I and K_{II} are the SIFs of mode-I and mode-II, respectively; ϕ_0 is the crack deflection angle.

Another criterion developed for mixed mode-I/II problems is the Richard criterion.[21,22] The equivalent SIF and crack deflection angle can be determined by the following equations:

$$K_{eq} = \frac{K_I}{2} + \frac{1}{2}\sqrt{K_I^2 + 4(\alpha_1 K_{II})^2} \leqslant K_{IC} \tag{3}$$

$$\phi_0 = \mp\left[155.5^\circ\frac{|K_{II}|}{|K_I| + |K_{II}|}\right] - 83.4^\circ\left[\frac{|K_{II}|}{|K_I| + |K_{II}|}\right]^2 \tag{4}$$

In Eq. (3), α_1 is a material parameter describing the ratio of K_{IC}/K_{IIC} and generally taken as 1.155.

Another criterion was proposed by Tanaka,[19] who stated a concept of the equivalent SIF for mixed mode conditions. According to this criterion, the equivalent SIF is formulated by

$$\Delta K_{eq} = \left[\Delta K_I^4 + 8\Delta K_{II}^4\right]^{1/4} \tag{5}$$

Pook[23] also developed an in-plane mixed mode criterion and proposed an equation from which the equivalent SIF can be obtained using mode-I and mode-II SIFs as

$$\frac{\Delta K_{II}}{\Delta K_{th}} = \left[0.08\left(\frac{\Delta K_I}{\Delta K_{th}}\right)^2 - 0.83\frac{\Delta K_I}{\Delta K_{th}} + 0.75\right]^{1/2} \tag{6}$$

where ΔK_{th} is the threshold range of stress intensity for mode-I.

In a previous study,[28] modeling and analysis of in-plane mixed mode-I/II fatigue crack growth experiments were carried out for each mode mixity ratio to evaluate the applicability of the equivalent SIF criterion developed for mixed mode-I/II fracture problems. The equivalent SIF equation with regard to the developed criterion[28] obtained using two types of specimens, namely CTS specimen and T-specimen, is given by

$$K_{eq} = \left(1.0519 \times K_I^4 - 0.035 \times K_{II}^4 + 2.3056 \times K_I^2 \times K_{II}^2\right)^{1/2} \tag{7}$$

3. Fatigue crack growth experiments

In this section, fatigue crack growth experiments are performed by using Compact Tension (CT) specimens under pure mode-I loading and by using CTS specimens under in-plane mixed mode loading. The Al 7075-T651 aluminum material, which has an elastic modulus of 70 GPa, a Poisson's ratio of 0.33, and an initial yield stress of 460 MPa, is machined from rolled plates in the L-T rolling direction and used for all experiments. Before fatigue crack growth experiments, fatigue pre-cracking is performed under mode-I loading according to the ASTM E647-13a standard[29] by using an axial fatigue test machine. Pre-crack lengths of all specimens used in experiments are determined as indicated in the standard. Crack propagation during tests is monitored and controlled by using a high-zoom camera and divided sub-millimetric scales on specimens, and the number of cycles are recorded simultaneously (see Fig. 1). Pre-crack and fatigue test loads are determined according to the ASTM condition $((K_{max})_{final\text{-}pre\text{-}cracking} \leq (K_{max})_{initial\text{-}testing})$. After generation of the pre-crack, fatigue crack growth tests are performed at $R = 0.1$ (where R is the stress ratio) for all experiments.

3.1. Mode-I fatigue crack growth experiments

In this sub-section, fatigue crack growth experiments are performed by using CT specimens (see Fig. 2) under pure mode-I loading to determine the fatigue crack growth rate data of the material used in the experiments.

The general fatigue crack growth behavior exhibited by most structural materials under constant-amplitude test conditions is described by the relationship between the crack growth rate, da/dN, and the stress intensity factor range, ΔK, in the lg-lg scale. In Fig. 3, a typical fatigue crack growth curve including three regions is shown. Paris and Erdogan[30] discovered the following equation for Region II, in which stable crack growth exists and logarithm of the crack growth rate linearly increases with increasing lg ΔK:

$$\frac{da}{dN} = C(\Delta K)^n \tag{8}$$

where C and n are crack growth-related material properties. ΔK is the SIF range and can simply be the mode-I SIF for mode-I loading conditions or an equivalent SIF, ΔK_{eqv}, for mixed mode crack growth situations. ΔK for a CT specimen under pure mode-I loading condition is calculated using the following formula according to the ASTM standard:

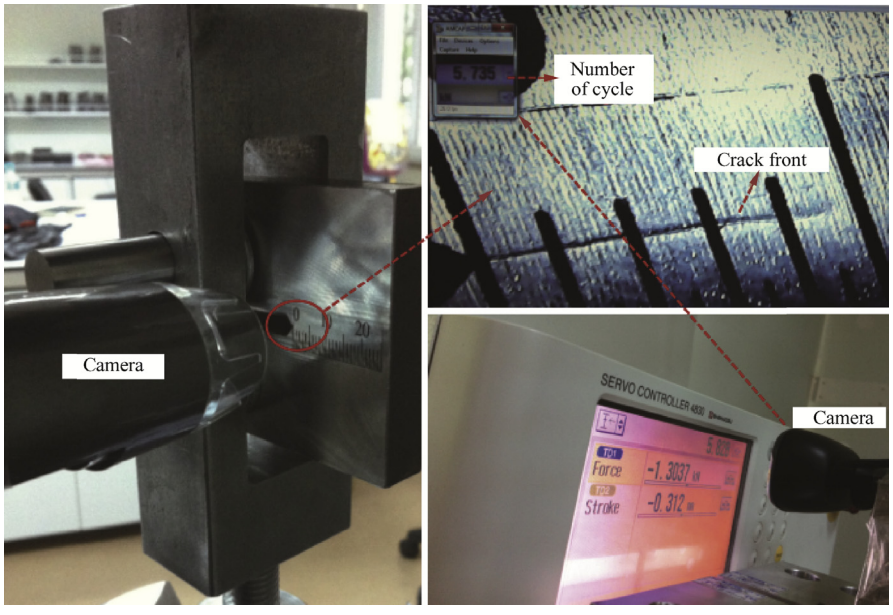

Fig. 1 Experimental set-up.

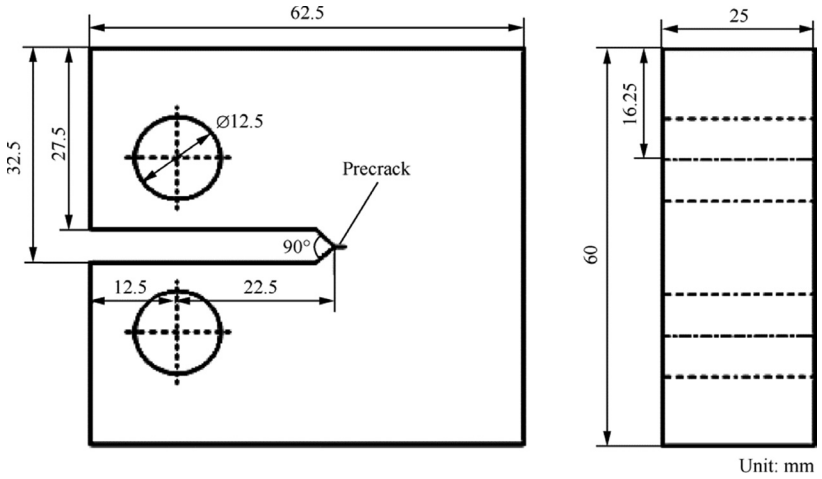

Fig. 2 Geometry and dimensions of a CT specimen.

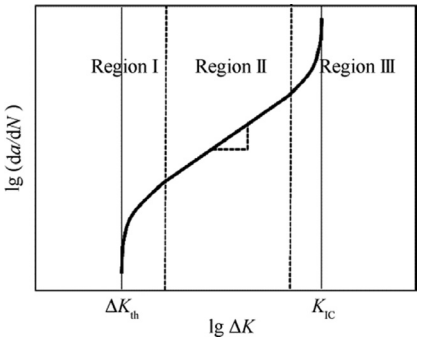

Fig. 3 Typical fatigue crack growth curve.

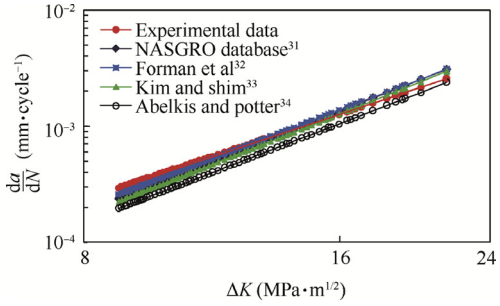

Fig. 5 Comparisons of fatigue crack growth rates for Al 7075-T651, $R = 0.1$.

$$\Delta K = \frac{\Delta P}{B\sqrt{W}} \frac{\left(2+\frac{a}{W}\right)}{\left(1-\frac{a}{W}\right)^{3/2}} \left[0.886 + 4.64\frac{a}{W} - 13.32\left(\frac{a}{W}\right)^2 + 14.72\left(\frac{a}{W}\right)^3 - 5.6\left(\frac{a}{W}\right)^4\right] \quad (9)$$

where ΔP is force range, a is crack length, B and W are the thickness and width of the specimen.

In Fig. 4, overall views of the CT specimens before and after tests are given. For each mode-I test, SIF ranges are calculated by using test load ranges and updated crack lengths based on crack growth increment measurements. Fatigue crack growth rate data of the material is plotted, and material constants C and n are obtained as 1.46×10^{-6} and 2.44, respectively (da/dN in "mm/cycle" and K in "MPa·m$^{1/2}$") by fitting the curves. Material constants obtained previously from the literature for Al 7075-T651 are substituted in Eq. (8), and the corresponding fatigue crack growth rate data are compared with the experimental data in the logarithmic scale (see Fig. 5). It is seen from the figure that experimental data obtained in this study are close to those from the literature.[31–34] Thus, for all mixed mode simulations presented in this paper, material properties obtained from mode-I fatigue

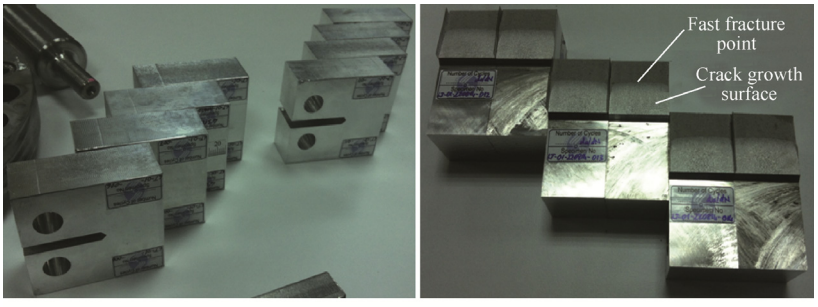

(a) Before test (b) After test

Fig. 4 Overall views of CT specimens before and after tests.

crack growth experiments are used to calculate crack propagation lives.

3.2. In-plane mixed mode-I/II fatigue crack growth experiments

In-plane mixed mode-I/II fracture experiments are performed under different loading angles using pre-cracked CTS specimens (see Fig. 6), which are widely used in the literature and proposed by Refs.[21,35].

Mixed mode loading apparatus are designed to allow the loading axis to pass through the mid-point of the specimen width under different loading angles. Fatigue crack growth experiments are carried out for loading angles of 30°, 45°, 60° and 75°. 10 mm thick specimens are used in the experiments. In Fig. 7, overall views of the experimental set-up are shown. The crack growth rates during load cycle intervals are recorded concurrently for each mixed mode loading condition. Consistent fracture surfaces and deflection angles are observed from the tests for all loading angles.

4. Modeling of fatigue crack growth experiments

Experimental fracture surfaces of all broken specimens are scanned exactly and the mean crack surface is obtained by a surface fit of the crack propagation planes for every mode mixity ratio, i.e., loading angle. Fracture surface regions, i.e., crack paths, are divided into equal spaces to model and analyze separately each incremental crack profile. Modeling and solution of the global problem, including all parts of the test system, for each mode mixity case are carried out using ANSYS™[36] by defining contact mechanics between the specimen and the loading apparatus. In Fig. 8, process steps involved in modeling of crack surfaces are shown representatively for the 9th crack propagation step under 30° loading angle. In an effort to simulate the real conditions as in the experiments, contacts are defined between the contact surfaces of the loading devices, pins and specimen. Boundary conditions are defined so that the surface nodes of the bottom loading clevis are constrained in all directions and those of the upper loading clevis are allowed to move along the loading axis only. Load is applied on the upper loading clevis in the vertical direction. Having obtained the overall global solution of the system using ANSYS™, displacements are taken from nodes of the loading hole surfaces of the specimen by using submodeling. Then, these displacements are applied on the specimen model, and three-dimensional fracture analyses are performed using FRAC3D, a standalone finite element program employing enriched finite elements to calculate the resulting SIFs as the main solver of FCPAS (Fracture and Crack Propagation Analysis System).[37,38] Having computed the mixed mode SIFs from the numerical analyses, equivalent SIFs on the crack fronts are calculated by substituting the SIFs (K_I and K_{II}) into the developed and existing mixed mode-I/II criteria, and life cycles are predicted for each criterion. Finally, crack propagation lives under different loading angles (30°, 45°, 60° and 75°) are compared with experimental results.

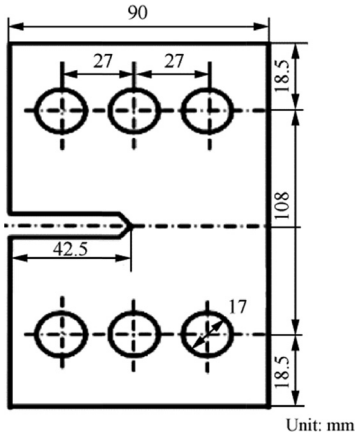

Fig. 6 Dimensions of a CTS specimen.[21,35]

5. Numerical and experimental results

In this section, results obtained from numerical analyses of actual mixed mode-I/II fatigue crack growth experiments and comparisons of fatigue crack growth rates predicted using different criteria with experimental results are presented for different loading conditions.

Three pre-cracked CTS specimens are tested experimentally under 30° loading angle. In an effort to ensure that the corresponding ASTM fatigue crack growth test condition $(K_{max})_{final\text{-}pre\text{-}cracking} \leq (K_{max})_{initial\text{-}testing}$ is satisfied, specimens are tested under two different fatigue test loads. An 8.8 kN fatigue load ($R = 0.1$) is applied to one specimen, labeled as CTS-01, and an 11 kN fatigue load ($R = 0.1$) is applied to the other two specimens, labeled as CTS-02 and CTS-03. In Fig. 9, front views of the broken specimens under the 30° loading angle are shown. Since fatigue pre-crack lengths measured after experiments are not always the same, in Fig. 9, fracture

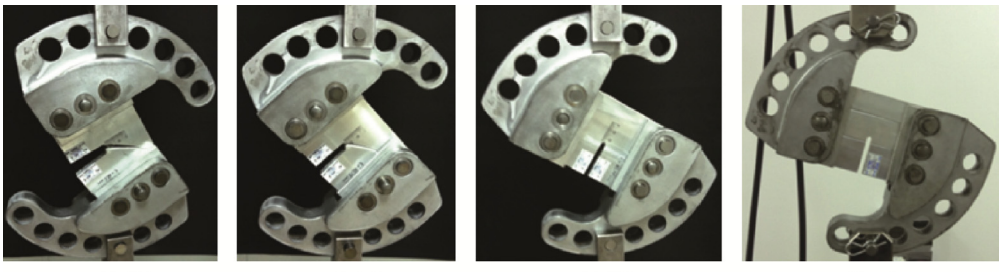

(a) 30° (b) 45° (c) 60° (d) 75°

Fig. 7 Overall views of experimental set-up with a CTS specimen under 30°, 45°, 60° and 75° loading angles.

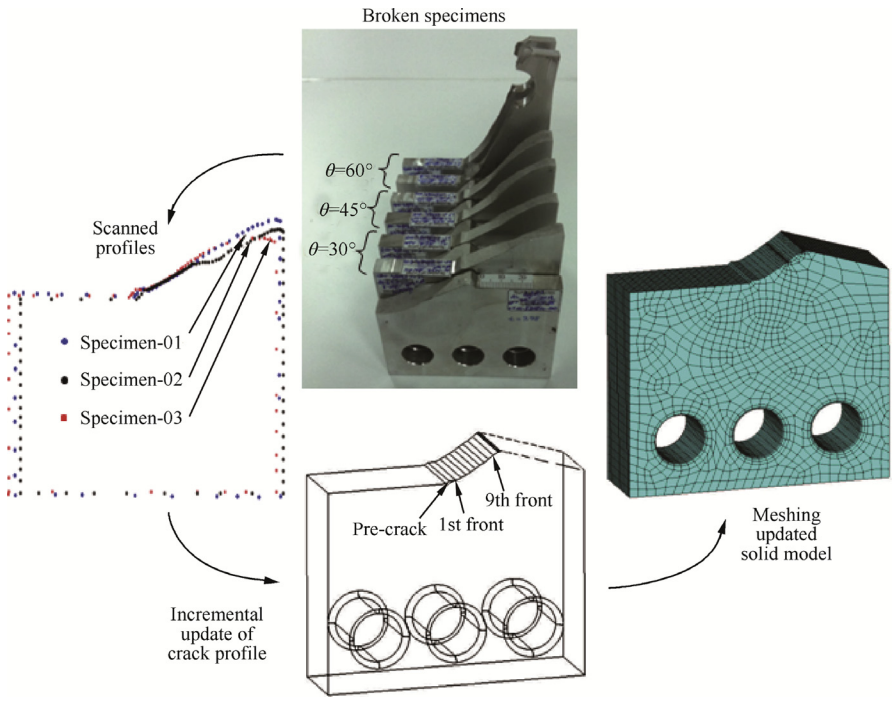

Fig. 8 Process steps involved in modeling of crack surfaces for the 9th crack propagation step under 30° loading angle.

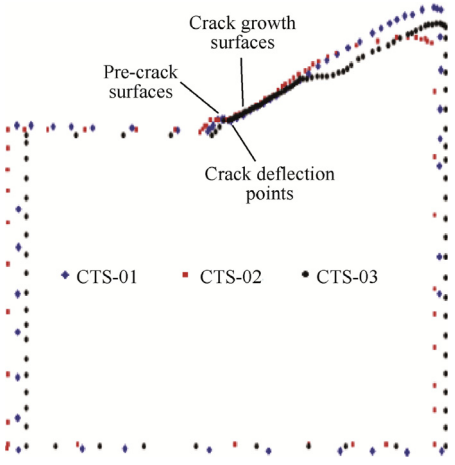

Fig. 9 Front views of three broken CTS specimens under 30° loading angle.

surfaces are overlapped at the crack deflection point of the fatigue pre-crack surface, and the mean crack deflection angle is obtained by surface fitting of the crack growth surfaces. Fracture analyses are performed by modeling the experimental crack surface for each crack propagation step until it reaches the starting point of unstable crack growth. In Table 1, SIFs obtained from center points of crack profiles and equivalent SIFs calculated using in-plane mixed mode-I/II criteria are given for the case of 8.8 kN fatigue loading.

Crack propagation lives are evaluated by substituting the equivalent SIFs into Eq. (8) for each criteria. Numerical analysis results for the 8.8 kN fatigue load are also scaled to represent the 11 kN fatigue load and to compare the results in terms of crack growth lives. Variations in crack length as a function of number of load cycles under the 30° loading angle are presented for 8.8 kN and 11 kN fatigue loads in Figs. 10(a) and (b), respectively. As can be seen from the figures, all of the criteria

Table 1 Predicted equivalent SIFs according to mixed mode-I/II criteria for 30° loading condition (applied load is 8.8 kN).

Crack profile number	SIFs (MPa·m$^{1/2}$) (center point)		Equivalent SIFs (MPa·m$^{1/2}$)				
	K_I	K_{II}	Richard criterion[21,22]	Erdogan and Sih criterion[14]	Pook criterion[23]	Tanaka criterion[19]	Developed criterion
Pre-crack	8.95	1.90	8.52	8.58	8.56	8.09	8.35
1st front	10.79	0.39	9.72	9.73	9.73	9.71	9.84
2nd front	11.75	−0.08	10.58	10.57	10.58	10.58	10.71
3rd front	12.74	−0.66	11.51	11.33	11.51	11.47	11.63
4th front	14.02	−0.59	12.64	12.51	12.65	12.61	12.79
5th front	15.13	−1.66	13.83	12.91	13.86	13.62	13.88
6th front	16.28	−1.07	14.74	14.37	14.75	14.65	14.88
7th front	17.42	−2.04	15.97	14.76	16.00	15.69	16.00
8th front	19.25	−2.30	17.65	16.27	17.68	17.33	17.68
9th front	21.08	−3.04	19.49	17.33	19.55	18.99	19.43

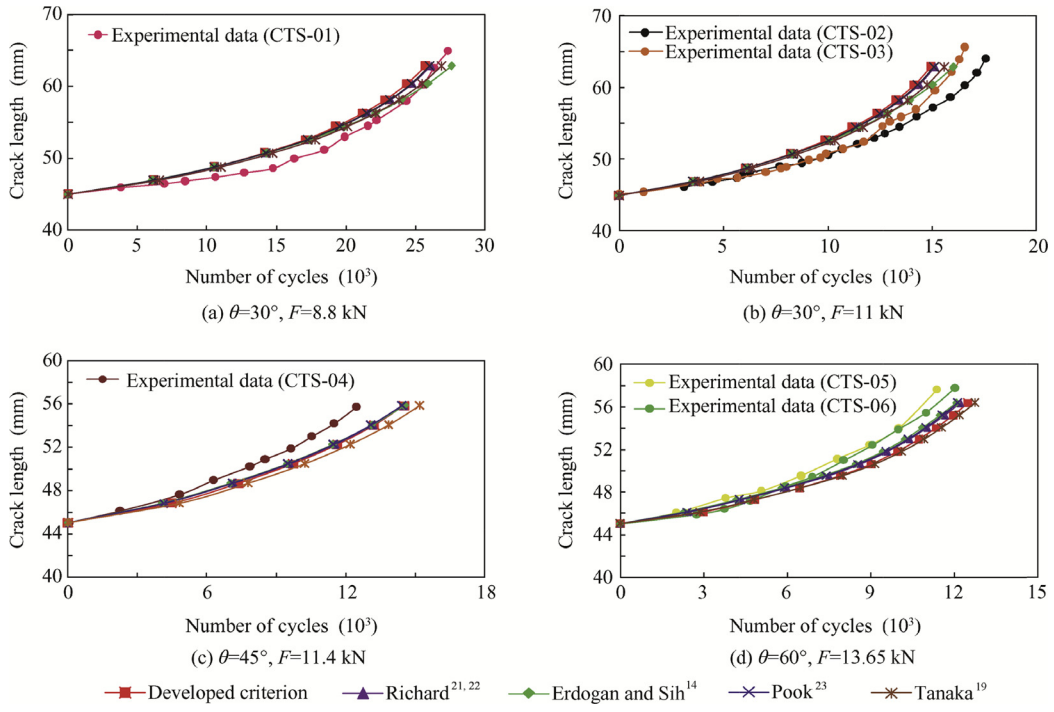

Fig. 10 Comparisons of fatigue crack growth lives predicted using different criteria and experimental data.

Table 2 Predicted equivalent SIFs according to mixed mode-I/II criteria for 45° loading condition (applied load is 11.4 kN).

Crack profile number	SIFs (MPa·m$^{1/2}$) (center point)		Equivalent SIFs (MPa·m$^{1/2}$)				
	K_I	K_{II}	Richard criterion[21,22]	Erdogan and Sih criterion[14]	Pook criterion[23]	Tanaka criterion[19]	Developed criterion
Pre-crack	8.95	3.21	9.26	9.46	9.36	8.31	8.68
1st front	12.77	0.75	11.55	11.55	11.55	11.49	11.66
2nd front	13.74	−0.03	12.37	12.37	12.37	12.37	12.52
3rd front	14.89	−0.27	13.40	13.38	13.40	13.40	13.57
4th front	16.15	−0.57	14.56	14.46	14.56	14.54	14.73
5th front	17.47	−0.89	15.78	15.54	15.78	15.72	15.94
6th front	18.81	−1.45	17.06	16.48	17.08	16.93	17.20

Table 3 Predicted equivalent SIFs according to mixed mode-I/II criteria for 60° loading condition (applied load is 13.65 kN).

Crack profile number	SIFs (MPa·m$^{1/2}$) (center point)		Equivalent SIFs (MPa·m$^{1/2}$)				
	K_I	K_{II}	Richard criterion[21,22]	Erdogan and Sih criterion[14]	Pook criterion[23]	Tanaka criterion[19]	Developed criterion
Pre-crack	7.79	5.04	9.83	10.36	9.99	8.73	8.35
1st front	12.40	1.18	11.29	11.31	11.31	11.16	11.35
2nd front	13.42	0.76	12.13	12.14	12.14	12.08	12.25
3rd front	14.24	0.78	12.87	12.87	12.87	12.82	13.00
4th front	14.97	1.35	13.62	13.64	13.63	13.48	13.71
5th front	16.47	0.37	14.83	14.83	14.83	14.82	15.01
6th front	18.08	−0.25	16.28	16.26	16.28	16.27	16.48
7th front	19.68	0.36	17.72	17.72	17.72	17.71	17.94
8th front	20.16	−0.87	18.19	18.00	18.20	18.15	18.40
9th front	21.35	−0.71	19.24	19.12	19.24	19.21	19.47
10th front	22.34	−1.43	20.21	19.74	20.23	20.10	20.41

agree very well with the experimental results under different fatigue loads.

Table 2 summarizes the SIFs from the fracture analyses performed for incremental crack propagation steps under 45° loading angle for the crack front center point on the crack front and the corresponding equivalent SIFs according to different mixed mode-I/II criteria. 11.4 kN fatigue loading is applied in the analyses. In Fig. 10(c), comparisons between predicted crack growth lives by different criteria and experimental lives for the 45° loading condition are given. All of the criteria have about the same and close tendency as the experimental results for this loading condition.

In Table 3, SIFs obtained for the crack front center point from the fracture analyses performed for incremental crack propagation steps under 60° loading angle and corresponding equivalent SIFs according to mixed mode-I/II criteria are presented. 13.65 kN fatigue loading is applied in the analyses. Crack lengths as a function of number of load cycles under the 60° loading angle are given in Fig. 10(d). Similar to other loading conditions, all of the criteria provide similar and close predictions to the experimental data.

Finally, fracture analyses are performed for incremental crack propagation steps under 75° loading angle. As is with the 30° loading case, 13 kN (R = 0.1) and 15 kN (R = 0.1) are applied separately in experiments and numerical analyses. In Fig. 11, distributions of SIFs along the crack front for each crack propagation step for the case of 15 kN fatigue loading under the 75° loading angle are given and the related equivalent SIFs computed for the crack front center point according to mixed mode-I/II criteria are given in Table 4. It is seen from Fig. 11 that, as expected, K_{II} and K_{III} decrease during crack growth while K_I increases, i.e., the mixed mode problem is converged to that of mode-I loading type, and eventually the crack continues to grow on a path perpendicular to the loading axis. The distribution of K_{III} SIFs along the crack front is linear due to the Poisson's ratio effect of the material.[28] It is also seen that the equivalent SIF obtained from the developed criterion[28] for the initial crack is much lower than that from the existing criteria. Although closer equivalent SIFs are obtained for lower mode mixity ratios using the developed and existing criteria, remarkable differences between them are observed for this loading angle.

As mentioned in the Section 1, most existing criteria show a deviation from experimental measurements under high mode mixity ratios according to some studies in the literature and a previous study.[28] Therefore, in the previous study,[28] a newly developed criterion involving highly mixed mode conditions was also proposed for in-plane mixed mode-I/II problems. Thus, significant differences are observed between existing criteria and the developed criterion for the initial crack in the 75° loading case. It is also seen that the equivalent SIFs for the later crack propagation steps are closer to each other. The reason is that, as the crack starts propagating under a mixed mode condition, the dominant mode type changes from mode-II to mode-I. SIF solutions obtained for the 15 kN fatigue load are scaled to represent the 13 kN fatigue load, and comparisons of crack growth lives predicted by criteria with experimental lives are given in Fig. 12. The closest trend is obtained between the prediction made by the developed criterion and experimental crack growth lives under the 13 kN fatigue load (see Fig. 12(a)). All of the criteria are in good agreement with the experimental results under the 15 kN fatigue load (see Fig. 12(b)). An acceptable level of agreement is seen between experimental results and numerical crack growth rates calculated by the developed criterion for both loading cases under the 75° loading angle.

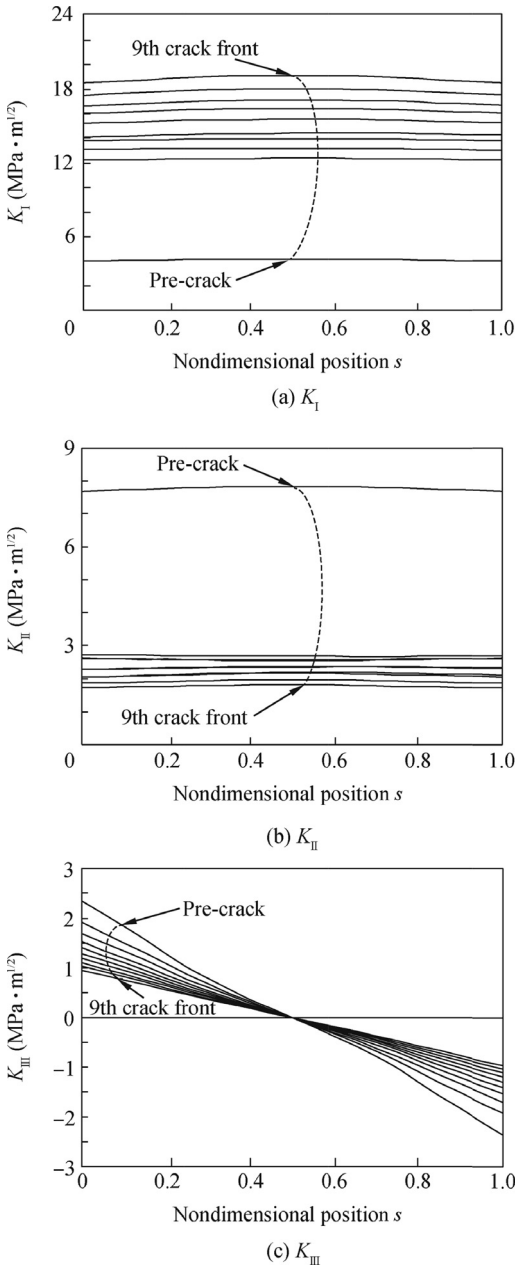

Fig. 11 Distributions of mixed mode SIFs along the crack front for each crack propagation step under 75° loading angle.

6. Summary

In this study, in-plane mixed mode-I/II fatigue crack growth experiments are performed under different loading conditions (30°, 45°, 60° and 75°), and modeling and analyses of the experiments are carried out to evaluate the applicabilities of a criterion developed previously by the authors and different criteria available in the literature to mixed mode-I/II crack growth tests. Results show that all of the criteria are in good

Table 4 Predicted equivalent SIFs according to mixed mode-I/II criteria for 75° loading condition (applied load is 15 kN).

Crack profile number	SIFs (MPaśm$^{1/2}$) (center point)		Equivalent SIFs (MPa·m$^{1/2}$)				
	K_I	K_{II}	Richard criterion[21,22]	Erdogan and Sih criterion[14]	Pook criterion[23]	Tanaka criterion[19]	Developed criterion
Pre-crack	4.15	7.84	10.25	11.64	10.38	11.89	6.44
1st front	12.36	2.68	11.79	11.88	11.85	11.17	11.55
2nd front	13.18	2.55	12.43	12.51	12.49	11.89	12.25
3rd front	13.96	2.58	13.12	13.19	13.17	12.60	12.96
4th front	14.41	2.34	13.41	13.47	13.46	12.99	13.32
5th front	15.54	2.36	14.41	14.46	14.45	14.00	14.34
6th front	16.40	2.19	15.10	15.15	15.14	14.77	15.09
7th front	17.10	2.16	15.71	15.75	15.74	15.39	15.72
8th front	18.03	1.96	16.48	16.51	16.50	16.23	16.54
9th front	19.10	1.81	17.39	17.42	17.41	17.19	17.49

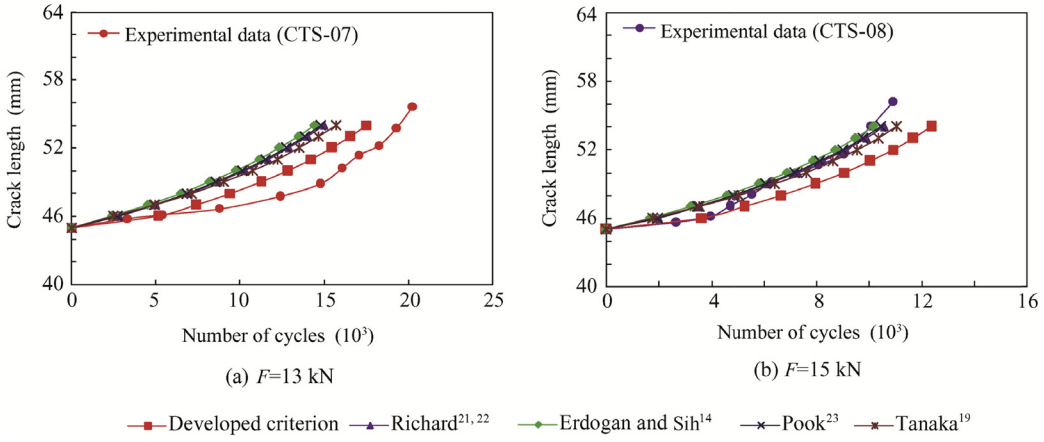

Fig. 12 Comparisons of fatigue crack growth lives predicted using different criteria and experimental data under 75° degree loading angle.

agreement with the experimental lives for all loading conditions. Although significant differences are obtained from the developed criterion in terms of equivalent SIFs for the initial crack, similar equivalent SIFs are obtained for the later crack propagation steps under 75° loading angle. Since a high mode mixity condition changes to almost nearly a mode-I condition immediately after the first crack propagation step from the initial crack, a significantly notable decrease is observed in K_{II}. Thus, closer crack growth lives are obtained between the used criteria and experimental data. Thus, crack growth lives are minimally affected by the difference obtained for the initial crack, yielding closer total crack growth lives between different criteria and experimental data.

Acknowledgements

This study was supported by the Scientific and Technological Research Council of Turkey (TUBITAK) (No. 113M407). The ability of usage of an axial fatigue test machine at Bursa Technical University is gratefully acknowledged.

References

1. Cowles BA. High cycle fatigue in aircraft gas turbines-an industry perspective. *Int J Fract* 1996;**80**(2–3):147–63.
2. Larsen JM, Worth BD, Annis Jr CG, Haake FK. An assessment of the role of near-threshold crack growth in high-cycle-fatigue life prediction of aerospace titanium alloys under turbine engine spectra. *Int J Fract* 1996;**80**(2–3):237–55.
3. Nicholas T, Zuiker JR. On the use of the Goodman diagram for high cycle fatigue design. *Int J Fract* 1996;**80**(2–3):219–35.
4. Salam I, Tauqir A, Khan AQ. Creep-fatigue failure of an aero engine turbine blades. *Eng Fail Anal* 2002;**9**(3):335–47.
5. Yee RK, Sidhu KS. Innovative laser heating methodology study for crack growth retardation in aircraft structures. *Int J Fatigue* 2005;**27**(3):245–53.
6. Molent L, Barter SA. A comparison of crack growth behaviour in several full-scale airframe fatigue tests. *Int J Fatigue* 2007;**29**(6):1090–9.
7. Zhuang W, Barter S, Molent L. Flight-by-flight fatigue crack growth life assessment. *Int J Fatigue* 2007;**29**(9):1647–57.
8. Jones R, Pitt S, Peng D. The generalised Frost-Dugdale approach to modelling fatigue crack growth. *Eng Fail Anal* 2008;**15**(8):1130–49.
9. Molent L, Barter SA. The lead fatigue crack concept for aircraft structural integrity. *Procedia Eng* 2010;**2**(1):363–77.
10. Zhuang W, Molent L. Analytical study of fatigue crack growth in AA7050 notched specimens under spectrum loading. *Eng Fract Mech* 2010;**77**(11):1884–95.
11. Molent L, Barter SA, Wanhill RJH. The lead crack fatigue lifing framework. *Int J Fatigue* 2011;**33**(3):323–31.
12. Haile M, Chen TK, Sediles F, Shiao M, Le D. Estimating crack growth in rotorcraft structures subjected to mission load spectrum. *Int J Fatigue* 2012;**43**:142–9.

13. Jones R, Tamboli D. Implications of the lead crack philosophy and the role of short cracks in combat aircraft. *Eng Fail Anal* 2013;**29**:149–66.
14. Erdogan F, Sih GC. On the crack extension of plates under plane loading and transverse shear. *J Basic Eng* 1963;**85**:519–27.
15. Sih GC. Strain energy density factor applied to mixed mode crack problems. *Int J Fract* 1974;**10**:305–21.
16. Hussain MA, Pu SU, Underwood J. Strain energy release rate for a crack under combined mode I and II. *ASTM STP* 1974;**560**:2–28.
17. Nuismer RJ. An energy release rate criterion for mixed mode fracture. *Int J Fatigue* 1975;**11**:245–50.
18. Chang KJ. On the maximum strain criterion-A new approach to the angled crack problem. *Eng Fract Mech* 1981;**14**: 107–24.
19. Tanaka K. Fatigue crack propagation from a crack inclined to the cyclic tensile axis. *Eng Fract Mech* 1974;**6**:493–507.
20. Sander M, Richard HA. Finite element analysis of fatigue crack growth with interspersed mode I and mixed mode overloads. *Int J Fatigue* 2005;**27**(8):905–13.
21. Sander M, Richard HA. Experimental and numerical investigations on the influence of the loading direction on the fatigue crack growth. *Int J Fatigue* 2006;**28**:583–91.
22. Richard HA, Schramm B, Schirmeisen N. Cracks on mixed mode loading-Theories, experiments, simulations. *Int J Fatigue* 2014;**62**:93–103.
23. Pook LP. The significance of mode I branch cracks for mixed mode fatigue crack growth threshold behaviour. In: Brown MW, Miller KJ, editors. *Biaxial and Multiaxial Fatigue*. London: Mechanical Engineering Publications; 1989. p. 247–63.
24. Biner SB. Fatigue crack growth studies under mixed-mode loading. *Int J Fatigue* 2001;**23**:259–63.
25. Zafosnik B, Ren Z, Ulbin M, Flasker J. Evaluation of stress 484 intensity factors using finite elements. Maribor, Slovenija: University of Maribor; 2000, Sept 11–12.
26. Qian J, Fatemi A. Mixed mode fatigue crack growth: a literature survey. *Eng Fract Mech* 1996;**55**(6):969–90.
27. Ren L, Zhu Z, Yang Q, Ai T. Investigation on the applicability of several fracture criteria to the mixed mode brittle fractures. *Adv Mech Eng* 2013;**2013**:1–11.
28. Demir O, Ayhan AO, İriç S. A new specimen for mixed mode-I/II fracture tests: Modeling, experiments and criteria development. *Eng Fract Mech* 2017;**178**:457–76.
29. ASTM E647–13a. Standard test method for measurement of 495 fatigue crack growth rates. West Conshohocken: ASTM Int; 496 2013.
30. Paris PC, Erdogan F. A critical analysis of crack propagation laws. *Trans ASME Ser D* 1963;**85**(4):528–33.
31. Sander M. Comparison of fatigue crack growth concepts with 500 respect to interaction effects. In: Nilsson F, editor. *15th European 501 Conference on Fracture (ECF15); 2004 Aug 11–13; Stockholm, 502 Sweden*. Amsterdam: European Structural Integrity Society; 2004.
32. Forman RG, Shivakumar V, Cardinal JW, Williams LC, McKeighan PC. *Fatigue crack growth database for damage tolerance analysis*. Washington, D.C.: Office of Aviation Research, U.S. Department of Transportation Federal Aviation Administration; 2005.
33. Kim JK, Shim DS. A probabilistic analysis on variability of fatigue crack growth using the markov chain. *KSME Int J* 1998;**12** (6):1135–42.
34. Abelkis PR, Potter JM. *Service fatigue loads monitoring, simulation, and analysis: a symposium (No: 671)*. West Conshohocken: ASTM Int; 1979. p. 94–117.
35. Richard HA, Benitz K. A loading device for the creation of mixed mode in fracture mechanics. *Int J Fract* 1983;**22**:55–8.
36. ANSYS. *Theory Manual Version 12.0*. Canonsburg: Ansys Inc; 2009.
37. Ayhan AO, Nied HF. Stress intensity factors for three-dimensional surface cracks using enriched elements. *Int J Numer Methods Eng* 2002;**54**:899–921.
38. Ayhan AO. Simulation of three-dimensional fatigue crack propagation using enriched finite elements. *Comput Struct* 2011;**89**(9–10):801–12.